

Diameter-Dependent Dispersion in Packed Cylinders

R. S. Maier

U.S. Army Engineer Research and Development Center, Vicksburg, MS 39180

D. M. Kroll

Dept. of Physics, North Dakota State University, Fargo, ND 58105

H. T. Davis

Dept. of Chemical Engineering and Materials Science, University of Minnesota, Minneapolis, MN 55455

DOI 10.1002/aic.11083

Published online January 3, 2007 in Wiley InterScience (www.interscience.wiley.com).

Keywords: porous media, transport, computational fluid dynamics, chromatography

The purpose of this note is to present new evidence of diameter-dependent dispersion in solute flowing through packed cylinders. Hydrodynamic dispersion was simulated at the pore scale in cylinders packed with spheres of diameter d , with cylinder radii ranging from $R = 5d$ to $R = 25d$. The time-dependent, axial dispersion coefficient, $D_L(t)$, was plotted for different cylinder radii. These plots cross over, implying diameter-dependent dispersion. Comparisons with periodic sphere packs suggest the cylinder wall introduces new scales of length and time for dispersion. These results were obtained from three-dimensional, pore-scale simulations of flow and transport in packed cylinders. The simulations are computationally demanding and we have been limited to relatively short durations. However, we were recently able to extend the duration enough to reveal the cross-over dynamics. We begin by describing the background for the new results.

Taylor dispersion¹ of a solute flowing in a tube illustrates the phenomenon of diameter-dependent dispersion. Taylor observed that radial variation in fluid velocity leads to an axial dispersion coefficient greater than the bulk molecular diffusivity, D_M , of the solute, and he showed that this coefficient develops over a time and distance that depend on the tube diameter and average velocity, v . Indeed, this result is general for arbitrary velocity profiles, as shown by Aris.² The packed column is similar, but requires the additional

consideration of the characteristic length scale of the porous medium.

It is generally accepted that the asymptotic axial dispersion coefficient in a packed cylinder depends on the ratio of cylinder diameter to particle diameter, $\beta = 2R/d$ because of near-wall packing effects on the velocity profile. Delgado³ reviews experimental investigations, dating to at least 1958, that discuss the effects of radial variations in porosity and velocity on dispersion. However, the consensus among these investigations is that dispersion is independent of the ratio for $\beta > k$, where k is a number in the range from 10 to 15. Gunn, for example, makes a case for diameter *independence* based on a mathematical model⁴ and earlier experimental results.⁵

De Ligny⁶ was perhaps the first to propose a correlation for the dispersion coefficient that explicitly accounts for both particle and cylinder diameters. The correlation predicts the effective dispersion coefficient in a packed cylinder from these two parameters and from the effective radial dispersion coefficient. The radial coefficient is assumed to be only weakly dependent on β .

A number of authors have developed models of radial variations in porosity and velocity and used them to predict concentration distributions and mass transfer zones in packed cylinders. Perhaps the simplest illustration is given by Rudraiah et al.⁷ for a rectangular packed duct; they assume Brinkman's equation to describe the near-wall velocity profile and further assume the value of a bulk dispersion coefficient that is characteristic of the

© 2007 American Institute of Chemical Engineers

*This article is a U.S. Government work and, as such, is in the public domain in the United States of America.

porous medium far from the wall. They predict the effective dispersion coefficient depends on duct size and is double that of the bulk dispersion coefficient in the large size limit. Tobis and Vortemeyer⁸ used models of radial variation in packed cylinders to predict dispersion and found significant diameter dependence even beyond $\beta > 100$. Our analysis supports their result.⁹

In summary, diameter-dependent dispersion has been observed in experiment only for fairly small values of β , whereas some numerical studies suggest stronger diameter dependence. A possible explanation for these differing conclusions may be found in the time scale for development of the dispersion coefficient and how they have been determined in previous experimental work.

The time scale for asymptotic development of axial dispersion in a tube is $t \sim R^2/D_M$, from Taylor dispersion. By analogy, the time scale for packed cylinders is $t \sim R^2/D_T$, where D_T is the coefficient of transverse dispersion. Kennedy and Jorgenson¹⁰ suggested a similar expression, $t \sim R^2/\gamma D_M$, where γ is a tortuosity factor. Han et al.¹¹ suggested the time scale, $t \sim d^2/D_M$, but this expression does not allow sufficient time for solute particles to traverse the cylinder radius and sample the wall region.

In some experiments, β is varied by changing the particle diameter in a column of fixed length, L , and radius. For a given particle Reynolds number, $Re = v\rho/d\mu$, the measurement time is therefore proportional to d . If D_L develops on a R^2/D_T time scale, it would be measured at a different stage of development for each choice of β . In other experiments, β is varied with cylinders of different radius but uniform length. In this case, the measurement time is equal for each choice of β , but the same concern would apply. Unless asymptotic dispersion has developed for each choice of β , one may question how preasymptotic behavior affects the comparison of different β ratios. Until recently, it has been difficult to obtain time-dependent dispersion coefficients to assess the development because it requires multiple sampling locations in a column. During the past decade, however, new experimental and simulation techniques have emerged that offer the possibility of determining dispersion at short time intervals.

Pore-scale simulations model the fluid and solid phases of a porous medium with geometric fidelity. Flow and transport are simulated in the fluid phase, yielding detailed three-dimensional velocity and concentration fields from which dispersion coefficients may be calculated. No assumptions about transport coefficients or average properties of the medium are required, except for the coefficients of solvent kinematic viscosity and solute molecular diffusion. The pore-scale simulations described in this note use three numerical methods.¹² The first is a Monte Carlo sphere-packing algorithm, used to generate three-dimensional random sphere packings in cylinders. The second method is a lattice-Boltzmann algorithm for single-phase, isothermal, low Mach-number flows in the pore spaces of the sphere packing. A regular grid, or lattice, is superimposed on the sphere packing and the fluid flow is simulated using only the grid cells in the pore spaces, with no-slip boundaries at the interfaces. The third method is a forward Euler implementation of the stochastic Langevin equation, used to calculate the trajectories of a large ensemble of tracer particles in the fluid flow field. (Fluid velocity is interpolated from the grid points to the individual tracer particles.) The grid cell spacing Δ is

selected so the sphere diameter $d \approx 25\Delta$; this yields acceptable accuracy for flow and transport calculations. The simulations are initiated with a uniform distribution of one tracer particle per fluid grid cell. For a packed cylinder of radius $R = 25d$ and length $L = 172d$, the grid dimensions were $1250 \times 1250 \times 4294$, the porosity of the sphere packing was 40%, and the number of tracer particles was two billion. Dispersion coefficients are obtained by simple moment calculations on the ensemble of tracer particle displacements in the pore-scale flow field. The time-dependent dispersion tensor is defined as $D(t) = (1/2)d\sigma^2/dt$, where $\sigma^2(t)$ denotes the covariance of the solute particle displacements.

Before describing the recent results on cross-over dynamics, we present a summary of earlier results¹² describing short-time behavior of the dispersion coefficient. In an unconfined sphere packing (one that has periodic boundaries in all three dimensions) $D_L(t)$ typically becomes asymptotic by $t \approx 10d/v$. Simulations of packed cylinders were previously completed for $t = 20d/v$, and $D_L(t)$ remains preasymptotic on this time scale. Initially, $D_L(t)$ increases faster in cylinders of smaller diameter. However, for $t > 10d/v$, $D_L(t)$ increases faster in cylinders of larger diameter. This implies a possible cross-over for $D_L(t)$ corresponding to cylinders of different radii.

In the present work, dispersion was simulated in a set of four cylinders, with radii $R = \{5d, 6.5d, 12.5d, 25d\}$ and $L \approx 160d$ with periodic ends. The cylinders were randomly packed with uniform spheres to a porosity of 40%. A steady flow solution with $Re = 1$ was computed in each cylinder under a uniform pressure gradient. A uniform concentration of tracer particles was released into the flow and their trajectories were computed according to the stochastic Langevin equation for a time of $t = 40d/v$. This time period is sufficiently short that the maximum distance traveled by any tracer particle is $< L$, preventing any recorelation with original position and velocity. The molecular diffusion coefficient was selected to yield a particle Peclet number of $Pe = v(d/D_M) = 476$. The spatial moments of the tracer particles were computed at short intervals and recorded in a file.

The time-dependent dispersion coefficient $D_L(t)$ is shown in Figure 1 for each packed cylinder. The behavior of the packed cylinders is clearly preasymptotic. A plot of $D_L(t)$ in an unconfined packing illustrates asymptotic behavior and is included for comparison.

The packed cylinder plots are all increasing, and the slope of $D_L(t)$ depends on R for $t > 10d/v$.

The plots of D_L vs. t for different cylinder radii cross over. The plot for $R = 6.5d$ overtakes that of $R = 5d$ at $t \approx 20d/v$. The plot for $R = 25d$ overtakes that of $R = 12.5d$ at $t \approx 35d/v$. The slopes for $R = 6.5d$ and $R = 12.5d$ are similar, but we expect the slope for $R = 6.5d$ to moderate sooner and be overtaken by the plots for $R = 12.5d$ and $R = 25d$. The expectation is that after further development, the magnitude of $D_L(t)$ would depend on R . In previous simulations we did not see a cross-over at $t \approx 20d/v$ for the same cylinder radii. This suggests that random packing variation can affect the slope of $D_L(t)$ at short times. We next describe a technique developed to extrapolate the pore scale results further in time.

We used a generalization of the Aris model of dispersion in a tube² to extrapolate the pore-scale simulations to the

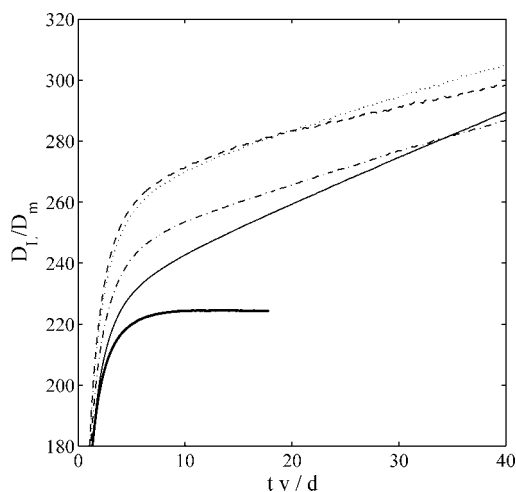


Figure 1. Pore-scale simulation results for dimensionless axial dispersion vs. dimensionless convective time in packed cylinders, $R = 25d$ (long solid curve), $R = 12.5d$ (dash-dot curve), $R = 6.5d$ (dotted curve), $R = 5d$ (dashed curve), and unconfined packing (short solid curve), for $Pe = 476$ ($Re = 1$).

asymptotic time scale. The idea is to use the radial variation in velocity from the pore-scale simulation in a simplified transport model.⁹ This model solves for the moments of the convection–diffusion equation in a packed cylinder. The radial component of velocity is assumed to be zero. The axial component of velocity is assumed to vary in the radial coordinate but is uniform in the axial coordinate. The radial velocity profile was computed from each of our pore-scale simulations (see Maier et al.^{9,12} for examples of such profiles). The model requires spec-

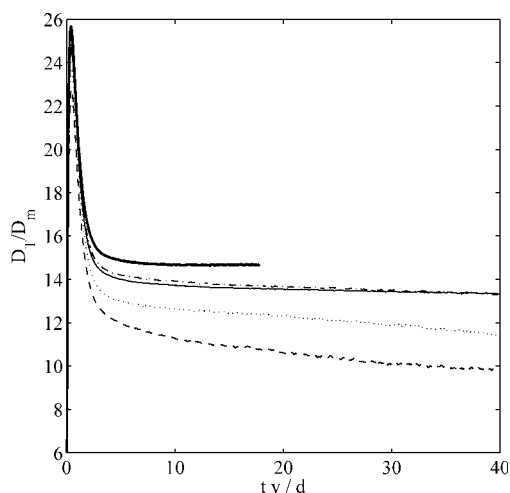


Figure 2. Pore-scale simulation results for dimensionless transverse dispersion vs. dimensionless convective time in packed cylinders, $R = 25d$ (long solid curve), $R = 12.5d$ (dash-dot curve), $R = 6.5d$ (dotted curve), $R = 5d$ (dashed curve), and unconfined packing (short solid curve), for $Pe = 476$ ($Re = 1$).

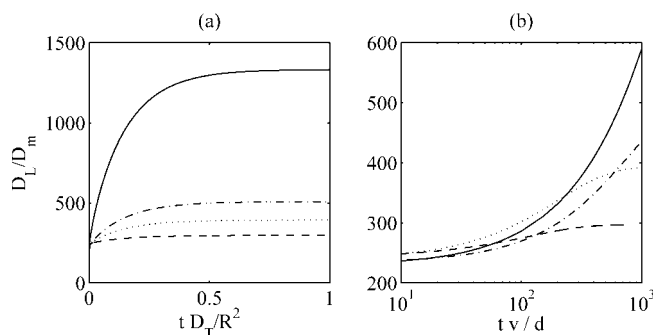


Figure 3. Extended Aris model of axial dispersion in packed cylinders.

(a) Asymptotic time scale, (b) convective timescale, $R = 25d$ (long solid curve), $R = 12.5d$ (dash-dot curve), $R = 6.5d$ (dotted curve), $R = 5d$ (dashed curve).

ification of a transverse dispersion coefficient and a bulk axial dispersion coefficient characteristic of the porous medium far from the wall, which we obtained from the unconfined packing shown in Figures 1 and 2. Thus, this is a qualitative model of how the radial velocity profile affects the development of asymptotic axial dispersion.

The extrapolations are shown in Figure 3. Figure 3a plots $D_L(t)$ on the cylinder time scale. The range is $R^2/D_T = 1$ and therefore represents a different physical time interval for each cylinder radius. However, on this time scale they each exhibit the same development toward their respective asymptotes. The asymptotic values are attained by $t \approx 0.3(R^2/D_T)$ and the magnitude of $D_L(t)$ depends on R .

Figure 3b plots dispersion on the convective time scale. The range is $t = 1000d/v$ and shows the cross-over region. This range represents the same physical time interval for each cylinder, but only a fraction of the R^2/D_T time scale for the larger ones. The plot for $R = 6.5d$ overtakes $R = 5d$ at $t \approx 10d/v$, compared to $t \approx 18d/v$ from pore-scale simulation. The plot for $R = 25d$ overtakes $R = 12.5d$ at $t \approx 15d/v$, compared to $t \approx 33d/v$ from pore-scale simulation. Figure 3b shows a number of other cross-overs beyond the pore-scale simulation time. A simple linear extrapolation of the plots in Figure 1 suggests the next cross-over would be $R = 25d$ and $R = 5d$ and, indeed, this is the next cross-over shown in Figure 3b, at $t \approx 60d/v$. The last cross-over, between $R = 12.5d$ and $R = 6.5d$, occurs at $t = 600d/v$.

It remains to be explained why previous experiments have demonstrated no significant diameter dependence for ratios of $\beta > 15$. One possibility is that experimental observation times correspond to the cross-over region, where diameter dependence is not easily inferred. Consider an experiment where the cylinder length is seven times the diameter and D_L is obtained from a breakthrough measurement at the cylinder outlet. In our simulations, $L = 350d$ is seven times longer than the diameter of our largest cylinder, $R = 25d$. The hypothetical breakthrough measurements would correspond to $t = 350d/v$ in Figure 3b, where cross-over dynamics somewhat obscure the diameter dependence. In Figure 3b, at $t = 350d/v$, the rank order of the four cylinders, from highest to lowest dispersion coefficient, is $R = \{25d, 6.5d, 12.5d, 5d\}$ with $D_L(t) = \{390, 370, 340, 290\}$, respectively.

Chromatographers have long suspected that very narrow cylinders ($R < 10d$) are more efficient, and both the experimental and simulation literature tend to support this idea. The pore-scale simulations suggest that cylinders of larger radius are apt to be even less efficient as their length is increased. We are extending these results to a wider range of flow rates, to determine in particular whether the same conclusions hold for the very low particle Reynolds number normally used in chromatographic investigations. We also expect to extend the results further in time with faster computers, as these become available, to simulate the entire cross-over region.

Acknowledgments

This work was strongly influenced by the late Emeritus Regents Professor Rutherford Aris, Dept. of Chemical Engineering and Materials Science, University of Minnesota. DMK acknowledges support from National Science Foundation Grant DMR-0513393.

Literature Cited

1. Taylor G. Dispersion of soluble matter in solvent flowing slowly through a tube. *Proc R Soc Lond A Phys Sci.* 1953;219:186–203.
2. Aris R. On the dispersion of a solute in a fluid flowing through a tube. *Proc R Soc Lond A Phys Sci.* 1956;235:67–77.
3. Delgado JMPQ. A critical review of dispersion in packed beds. *Heat Mass Transfer.* 2006;42:279–310.
4. Gunn DJ, Pryce C. Dispersion in packed beds. *Trans IChemE.* 1969;47:T341–T350.
5. Gunn DJ. Axial and radial dispersion in fixed beds. *Chem Eng Sci.* 1987;42:363–373.
6. De Ligny CL. The contribution of eddy diffusion and of the macroscopic mobile phase velocity profile to plate height in chromatography. *J Chromatogr.* 1970;49:393–401.
7. Rudraiah N, Pal D, Vortmeyer D. The effect of aspect ratio on longitudinal diffusivity of a porous medium of rectangular cross-section. *Int Commun Heat Mass Transfer.* 1985;12:313–322.
8. Tobis J, Vortmeyer D. Scale-up effects due to near-wall channeling in isothermal adsorption columns: On the limitations in the use of plug flow models. *Chem Eng Process.* 1991;29:147–153.
9. Maier RS, Kroll DM, Bernard RS, Howington SE, Peters JF, Davis HT. Enhanced dispersion in cylindrical packed beds. *Philos Trans R Soc Lond A Phys Sci.* 2002;360:497–506.
10. Kennedy RT, Jorgenson JW. Preparation and evaluation of packed capillary liquid chromatography columns with inner diameters from 20 to 50 μm . *Anal Chem.* 1989;61:1128–1138.
11. Han NW, Bhakta J, Carbonell RG. Longitudinal and lateral dispersion in packed beds: Effect of column length and particle size distribution. *AIChE J.* 1985;31:277–288.
12. Maier RS, Kroll DM, Bernard RS, Howington SE, Peters JF, Davis HT. Hydrodynamic dispersion in confined packed beds. *Phys Fluids.* 2003;15:3795–3815.

Manuscript received Aug. 24, 2006, and revision received Oct. 23, 2006.